DALTON
FULL PAPER

Anodic oxidation of molybdenum and tungsten in alcohols: isolation and X-ray single-crystal study of side products

Vadim G. Kessler,*,†,[a] Andrei N. Panov,[a] Nataliya Ya. Turova,[a] Zoya A. Starikova,[b] Alexandr I. Yanovsky,[b] Fedor M. Dolgushin,[b] Alexandr P. Pisarevsky[b] and (the late) Yuri T. Struchkov[b]

[a] *Chemistry Department, Moscow State University, 119899 Moscow, Russia*
[b] *A. N. Nesmeyanov Institute of Organoelement Compounds, Vavilov St. 28, 117813 Moscow, Russia*

The study of the side products of the anodic dissolution of molybdenum and tungsten metals in alcohols in the presence of LiCl showed them to be $[LiMo_2O_2(OMe)_7(MeOH)]$ **1** in the case of MeOH and $[LiMo_2O_4(OEt)_5(EtOH)]$ **2** in EtOH. Treatment of **2** with an excess of Pr^iOH gave $[LiMo_2O_4(OPr^i)_5(Pr^iOH)]$ **3**, the structure of which was confirmed by a study of $[\{LiMo_2O_4(OPr^i)_4(OC_2H_4OMe)\}_2]$ **4**, the product of partial substitution of OR groups in **3** by 2-methoxyethoxide ligands. Reaction of **2** with an excess of $MeOC_2H_4OH$ led to an equimolar mixture of $[MoO_2(OC_2H_4OMe)_2]$ and $[LiMoO_2(OC_2H_4OMe)_3]$ **5**. In Pr^iOH a crystalline product identified as $[Mo_6O_{10}(OPr^i)_{12}]$ **6** was isolated. Anodic oxidation of tungsten in MeOH gave a mixture of homometallic $W(OMe)_6$ and $[WO(OMe)_4]$. Electrosynthesis in EtOH gave as major product an amorphous glass-like mass {after separation of crystalline $[WO(OEt)_4]$ by filtration and subsequent drying of the filtrate *in vacuo*}. Treatment of the latter with an excess of HOC_2H_4OMe led to crystallization of $[\{LiWO_2(OC_2H_4OMe)_3\}_2 \cdot 2Li(HOC_2H_4OMe)_2]^{2+}[W_6O_{19}]^{2-}$ **7**. Complexes **1**, **4** and **7** were characterized by X-ray single-crystal studies. A GLC-mass spectrometric study of the composition of organic side products indicated that the processes were associated with formation of ethers, alkyl halides, aldehydes or ketones and their derivatives. The nature of the possible side reactions was deduced on the basis of the data obtained.

The chemistry of metal alkoxides is of interest because of the prospect of their large-scale application as precursors of oxide materials for modern technology.[1] The anodic oxidation of metals in anhydrous alcohols in the presence of conductive additives (alkali-metal halides) was developed to meet its requirements.[2,3] Earlier we reported the application of this method for the synthesis of the alkoxides of molybdenum and tungsten.[4–7] The main products of this reaction were $[MO(OR)_4]$. The formation of oxo complexes was due mainly to the propensity of molybdenum and tungsten derivatives $M(OR)_6$ to decomposition with elimination of ethers,[4,7] equation (1). When $[NBu_4]Br$ was taken in high concentration

$$M(OR)_n \xrightarrow{\text{heat}} MO(OR)_{n-2} + R_2O \qquad (1)$$

as conductive additive after a long electrolysis of tungsten in EtOH the product of complete decay, $[NBu_4]_2[W_6O_{19}]$, was isolated.[5] The formation of oxo complexes was considered to be caused also by cathodic reduction of the initially formed hexavalent alkoxide and subsequent oxidation of reduction products by traces of oxygen (from the atmosphere or dissolved in the solvents applied),[8,9] equations (2) and (3). The reddish

$$\text{Cathode: } M(OR)_n + e \longrightarrow M(OR)_{n-1} + RO^- \qquad (2)$$

$$M(OR)_{n-1} + \tfrac{1}{2}O_2 \longrightarrow MoO(OR)_{n-2} + RO^{\bullet} \qquad (3)$$

brown coloration observed in the course of electrolysis was consistent with this supposition. Its intensity under comparable conditions increased with the size and branching of the radical in the series $Me \ll Et < Pr^i$, while the speed of discoloration of electrolytes in dry air decreased in the same series. The formation of a red crystalline product was observed on anodic dissolution of the metal in Pr^iOH. It was described as $[Mo_5O_7(OPr^i)_8]$ {by analogy with $[Mo_5O_7(OH)_8]$, 'molybdenum blue', possessing the same color}.[4] Anodic dissolution of both molybdenum and tungsten metals in a functional alcohol, 2-methoxyethanol, led to the formation of brightly colored products, which were practically stable to oxidation.[7,10] The yields of $[MO(OR)_4]$ (M = Mo, R = Me, Et or Pr^i;[4] M = W, R = Me or Et[5]) were in all cases far from quantitative and therefore it was interesting to examine the composition of the side products and try to understand the mechanisms of processes taking place and improve the synthesis of pure products.

Experimental

All compounds described in this work are highly sensitive to moisture and oxygen and therefore all operations with them were carried out either using a vacuum line or a dry-box.

Dehydration of alcohols, ROH, used was performed by boiling them under reflux over magnesium (R = Me or C_2H_4OMe), calcium (R = Et) and aluminium ($R = Pr^i$) alkoxides with subsequent distillation. Toluene and hexane were refluxed with sodium wire and then distilled over $LiAlH_4$. Pyridine was stored over anhydrous KOH and distilled over a fresh portion of KOH prior to use.

The carbon and hydrogen contents of the samples were determined using the conventional combustion technique. Molybdenum and tungsten contents were determined gravimetrically as MO_3. Hydrated oxides were precipitated from solutions by hot 1:1 diluted HNO_3, washed with deionized water on the filter and heated to constant weight at 400 °C. The lithium content was determined by flame photometry with a FLAPHO-4 device.

Infrared spectra were registered with a Specord IR 75 for Nujol or hexachlorobutadiene mulls. Crystalline solids were identified using powder diffractometry (DRON 3M). The GLC–mass spectrometry tests were carried out using a Varian MAT 311A device (source temperature 200 °C, SE-30 separation column).

† *Permanent address*: Chemistry Department, Swedish University of Agricultural Sciences, Box 7015, S-75007 Uppsala, Sweden.

Table 1 Main parameters of the electrochemical synthesis of molybdenum and tungsten alkoxides

Alcohol	Material of anode/cathode	*E*/V	[LiCl]/mol dm^{-3}	*t*/h	Final Li : M ratio in the electrolyte	Products, isolable from electrolyte	Yield (%) in relation to metal dissolved	Organic side products detected
MeOH	Mo/Mo	110	0.076	12	1 : 4.92	$[MoO(OMe)_4]$	71	None
						$[LiMo_2O_2(OMe)_7(MeOH)]$	17	
EtOH	Mo/Pt	110	0.50	18	1 : 0.87	$[MoO(OEt)_4]$	82	EtCl, Et_2O
						$[LiMo_2O_4(OEt)_5(EtOH)]$	15	$MeCH(OEt)_2$
Pr^{i}OH	Mo/Mo	220	0.05	12	1 : 0.49	$[MoO(OPr^i)_4]$	46	Pr^{i}Cl, Me_2CO
						$[Mo_6O_{10}(OPr^i)_{12}]$	17	$Pr^i{}_2O$
MeOH	W/Pt	110	0.021	12	1 : 8.46	$W(OMe)_6$	81	None
						$[WO(OMe)_4]$	17	
EtOH	W/Pt	110	0.47	30	1 : 0.83	$[WO(OEt)_4]$	28	EtCl, Et_2O, MeCHO

Synthesis and isolation of the products obtained

The anodic oxidation of metals was carried out in a standard cell with an undivided cathodic and anodic space, supplied with water cooling; the anodes were plates of molybdenum or tungsten (≈20 cm^2) and the cathodes were plates of the same metals or platinum having the same size.[3] The parameters of the processes are summarized in Table 1.

$[LiMo_2O_2(OMe)_7(MeOH)]$ 1. The wine-red electrolyte prepared by dissolution of molybdenum in MeOH (≈100 cm^3) containing LiCl was concentrated to 1/10 of the initial volume and cooled to 0 °C. The precipitate formed was separated by decantation and washed twice with cold MeOH (5 cm^3). From the orange crystalline product obtained (8.64 g, 88% in relation to molybdenum metal dissolved), $[MoO(OMe)_4]$ was extracted by three portions (each 50 cm^3) of hot (50 °C) hexane. The extracts were mixed with each other and after evaporation in vacuum gave a yellow powder (6.26 g, 71%), identified as $[MoO(OMe)_4]$ using IR and X-ray powder data (see ref. 6). The residue after extraction, a bright reddish orange powder, was recrystallized from the minimum volume of MeOH, which was then cautiously evaporated in vacuum to dryness giving bright red needles. Yield 2.37 g (17%) (Found: C, 19.71; H, 5.06; Li, 1.38; Mo, 40.8. Calc. for $C_8H_{25}LiMo_2O_{10}$: C, 20.02; H, 5.21; Li, 1.36; Mo, 40.0%). IR (cm^{-1}): 3533m, 3360s (br), 1453s, 1412m, 1351m, 1154w, 1140 (sh), 1080m, 1046s, 1005s, 916s,* 894s,* 569s and 500s (br).‡

$[LiMo_2O_4(OEt)_5(EtOH)]$ 2. The attempts to crystallize the ethoxide analog of compound **1** being unsuccessful and observing the continuous decoloration of the electrolytes even in an inert atmosphere, we decided to subject the solutions to oxidation. The reddish brown electrolyte obtained was thus left for 2 d in a vessel connected to the atmosphere *via* a column filled with dry molecular sieves (4 Å). Its color then slowly changed to yellowish brown. The solution obtained was concentrated in vacuum and $[MoO(OEt)_4]$ was extracted by hexane from the liquid residue formed, using the technique described[4] (10.42 g, 82%). The residue from the extraction, a yellowish brown viscous liquid, was left for crystallization. After a week the formation of slightly yellowish transparent crystals was observed. They were separated from the mother-liquor by decantation and dried in vacuum. Yield 1.91 g (15%) (Found: C, 26.06; H, 5.93; Li, 1.23; Mo, 36.5. Calc. for $C_{12}H_{31}LiMo_2O_{10}$: C, 26.99; H, 5.81; Li, 1.22; Mo, 36.0%). IR (cm^{-1}): 3406s (br), 1273w, 1160m, 1097s, 1052s (br), 954 (sh),* 940s,* 920s,* 887s (br),* 814w,* 614w, 558s (br), 471m and 427w.

$[LiMo_2O_4(OPr^i)_5(Pr^iOH)]$ 3. To a portion of the crystals of compound **2** (≈0.5 g) was added Pr^{i}OH (20 cm^3) and after the dissolution was completed the solvent was removed in vacuum. The operation was repeated twice. The residue finally obtained was a viscous yellowish brown matter displaying rather high solubility in hexane and Pr^{i}OH. After approximately 3 d of storage in a refrigerator at 0 °C the formation of nearly colorless transparent crystals was observed. It was practically impossible to separate them properly from the surrounding amorphous matrix, which eventually precluded reliable microanalysis data or determination of the yield. The IR spectrum was registered for a single crystal cleaned manually (cm^{-1}): 3400s (br), 1170m, 1125 (sh), 1110s, 1067m, 1035m, 1010w, 980s,* 930s (br),* 901s,* 885s,* 845m,* 826m,* 817m,* 600s and 475m.

$[LiMo_2O_4(OPr^i)_4(OC_2H_4OMe)]$ 4. To a portion (1 g, ≈1.6 mmol) of the product obtained above was added hexane (10 cm^3) and then $MeOC_2H_4OH$ (0.2 g, 2.6 mmol). The system immediately separated into two liquid phases and in a week colorless transparent crystals grew from the lower layer. The yield was 0.82 g (88%) (Found: C, 32.16; H, 6.29; Li, 1.1; Mo, 33.1. Calc. for $C_{15}H_{35}LiMo_2O_{10}$: C, 31.38; H, 6.10; Li, 1.13; Mo, 33.5%). IR (cm^{-1}): 1366s, 1348w, 1330w, 1264w, 1239w, 1199w, 1167m, 1129s, 1108vs, 1060s, 1015m, 964 (sh),* 936vs (br),* 908s,* 893s,* 878 (sh),* 848m,* 833m,* 822m,* 612s, 602s, 551w, 481m, 455m (br), 421w and 394m.

$[LiMoO_2(OC_2H_4OMe)_3]$ 5. To this residue from the $[MoO(OEt)_4]$ extraction from the corresponding electrolyte, containing an estimated 2.5 g of compound **2**, was added $MeOC_2H_4OH$ (20 cm^3) and the mixture was heated to 60 °C, and then the solvent was evaporated to dryness in vacuum. This operation was repeated twice and the residual viscous dark matter left for crystallization which occured in 2–3 h with the formation of crystals of two types, bulky prisms and thin needles. On addition of $MeOC_2H_4OH$ (4 cm^3) and heating to 40 °C the needles dissolved completely. The residue consisted of 0.61 g of prismatic crystals found to be $[MoO_2(OC_2H_4OMe)_2]$ from the IR and microanalysis data (see ref. 10). On cooling the above-mentioned solution the precipitation of needle-shaped crystals of compound **5** occurred (Found: C, 20.64; H, 4.06; Li, 1.91; Mo, 26.1. Calc. for $C_9H_{21}LiMoO_8$: C, 20.00; H, 3.89; Li, 1.94; Mo, 26.67%). IR (cm^{-1}): 1105s, 1052s, 1024s, 1000s, 964w,* 898s,* 870s,* 846s,* 820s,* 800s,* 600s, 550s, 515m, 485s and 425s.

Compound **5** was also synthesized on saturation of 10% $LiOC_2H_4OMe$ solution (3 g) (prepared by dissolution of lithium metal in $MeOC_2H_4OH$) with solid $[MoO_2(OC_2H_4OMe)_2]$ (1.02 g) (prepared according to ref. 10). Compound **5** (0.81 g, 61%) precipitated after the mixture had been kept overnight at room temperature.

$[Mo_6O_{10}(OPr^i)_{12}]$ 6. The mixture obtained by dissolution of molybdenum in Pr^{i}OH consisted of two different products, a yellowish brown solution {from which, after the evaporation of

‡ Characteristic bands in the M–O and C–C vibration region are indicated by an asterisk.

solvent in vacuum, $[MoO(OPr^i)_4]$ containing variable amounts of Li according to microanalysis and thus polluted by compound **3** can be extracted by hexane} and reddish orange crystals. The latter are practically insoluble in the electrolyte on heating. They do not possess any noticeable solubility either in Pr^iOH or hexane and are relatively stable to oxidation in a dry atmosphere. We have earlier erroneously described them as $[Mo_5O_7(OPr^i)_8]$ by analogy with the $[Mo_5O_7(OH)_8]$ 'molybdenum blue' possessing the same color.[4] In the present work we compared the microanalytical and IR spectral data for this product with those given[9] for $[Mo_6O_{10}(OPr^i)_{12}]$ (Found: C, 28.85; H, 5.61; Mo, 40.4. Calc. for $C_{36}H_{84}Mo_6O_{22}$: C, 29.92; H, 5.82; Mo, 39.9%). IR (cm^{-1}): 1319m, 1140m, 1118m, 1099s, 986s,* 953s,* 930vs,* 850m,* 842m,* 800s (vbr),* 618 (sh), 605s, 555m, 500 (sh) and 473m.

The obtained crystals of compound **6** demonstrate the same chemical properties as those described for $[Mo_6O_{10}(OPr^i)_{12}]$ in ref. 9: they are perfectly soluble in toluene, but cannot be crystallized out again from this solution by either cooling or evaporation of the solvent; the latter yields a viscous reddish brown liquid. The addition of dry pyridine (py) to the mentioned solution leads to precipitation of a red crystalline powder of $[Mo_4O_8(OPr^i)_4(py)_4]$ as has been described[9] for the discussed compound.

Anodic oxidation of tungsten in methanol. The reddish orange electrolyte (≈100 cm^3) was evaporated in vacuum practically to dryness and the residue extracted by hexane (50 cm^3). The extract had a dark blue color which soon disappeared. When dried in vacuum it gave a colorless crystalline product identical with that described[5] and thus being a mixture of $W(OMe)_6$ and $[WO(OMe)_4]$ (see Table 1).

Anodic dissolution of tungsten in ethanol; isolation of $[\{LiWO_2(OC_2H_4OMe)_3\}_2{\cdot}2Li(MeOC_2H_4OH)_2]^{2+}[W_6O_{19}]^{2-}$ 7. The wine-red electrolyte obtained was left for 2 d in contact with the atmosphere *via* a column filled with molecular sieves which made it colorless. From this colorless solution thin needle-shaped crystals crystallized in 2 d. They were filtered off, washed on the filter by two portions of EtOH (each 10 cm^3) and dried in vacuum. This gave 4.16 g (28%) of a product identified as $[WO(OEt)_4]$ by IR and microanalysis (see ref. 11). Evaporation of the filtrate gave ≈11 g of a colorless amorphous glass-like matter. It was mixed with $MeOC_2H_4OH$ (40 cm^3), heated to 60 °C and then dried in vacuum. This procedure was repeated twice and the colorless liquor obtained was layered with hexane (30 cm^3). After approximately 18 h large irregularly shaped crystals crystallized; yield 6.41 g, ≈50% (Found: C, 13.81; H, 2.87; Li, 1.01; W, 55.9. Calc. for $C_{30}H_{74}Li_4O_{43}W_8$: C, 13.73; H, 2.82; Li, 0.99; W, 56.15%). IR (cm^{-1}): 1352s, 1290m, 1280w, 1265 (sh), 1245m, 1204s, 1130s (br), 1110m, 1092 (sh), 1070s, 1036s, 1016s, 982m,* 940s,* 918vs,* 900vs,* 876s*, 820s,* 625s, 578s, 566s, 535s, 508s, 465s and 410m.

Crystallography

All compounds studied are extremely sensitive to the ambient atmosphere and therefore were placed in glass capillaries, sealed under an inert atmosphere for data collection. The crystal data and experimental conditions are presented in Table 2. All calculations were performed on an IBM personal computer using SHELXTL PLUS programs (Version 4 for **4**, Version 5 for **1** and **7**).[12] All structures were solved by direct methods and refined by the full-matrix least-squares technique. All H atoms in **1** were located in the Fourier-difference synthesis and refined in the isotropic approximation. The positions of hydrogen atoms in **4** and **7** [with the exception of those of hydroxyl groups, *i.e.* atoms H(10) and H(12) in **7**] were calculated geometrically and included in the refinement in isotropic approximation for **4** and using the riding motion model for **7**; the thermal parameters for H atoms in **7** were taken as $U_{iso} = 1.2U_{eq}$(C) for those in CH and CH_2 groups and $1.5U_{eq}$(C) for those of CH_3 groups, where U_{eq}(C) was the equivalent parameter for the carbon atom to which the hydrogen atom is attached. Atoms H(10) and H(12) in **7** were located in the Fourier-difference syntheses and thereafter refined using the riding motion model; the U_{iso} values were taken as $1.2U_{eq}$(O), where U_{eq}(O) was the equivalent parameter for the O(10) and O(12) atom respectively.

CCDC reference number 186/752.

For crystallographic files in CIF format see http://www.rsc.org/suppdata/dt/1998/21/.

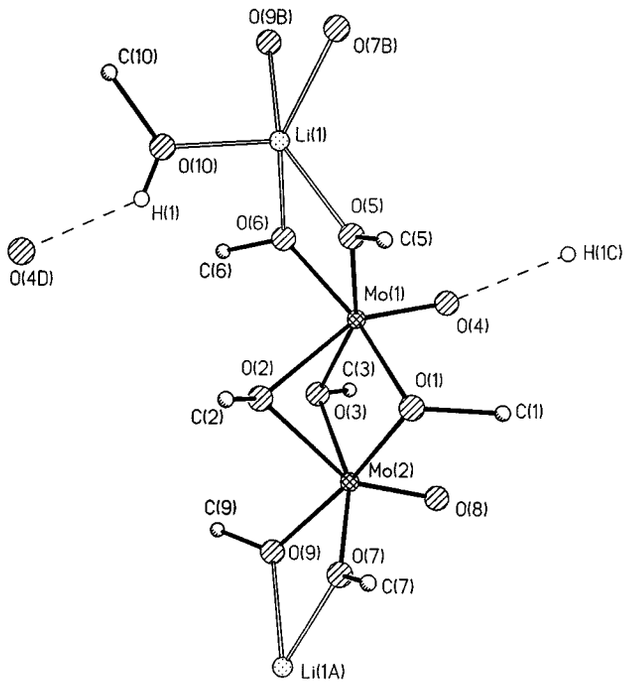

Fig. 1 Structure of a fragment of the polymeric chain in the crystal of compound **1**. Atoms derived from the reference atoms by symmetry operations are denoted by capital letters: A $x + 1, y, z$; B $x - 1, y, z$; C $x, 0.5 - y, z - 0.5$; D $x, 0.5 - y, z + 0.5$

Results and Discussion

Molecular and crystal structures

The structure of compound **1** can be most naturally considered as consisting of anionic $[Mo_2O_2(OMe)_7]^-$ and cationic $[Li(MeOH)]^+$ fragments bound in infinite chains parallel to the *a* axis; a fragment of the chain is shown in Fig. 1; see also Table 3. The hydrogen bonds which occur between the OH group H(1)–O(10) of the solvating MeOH molecule and one of the oxygen atoms O(4) connect the chains into layers parallel to the *ac* plane [O(10)···O(4D) 2.911(5), O(10)–H(1) 0.91(11), H(1)···O(4D) 2.17 Å, O(10)–H(1)–O(4D) 139(9)°].

The anionic fragment in the crystal of compound **1** is an example of the M_2X_9 group which is very widespread in the chemistry of metal alkoxides and halides and consists of two octahedra sharing a common face. Such an isolated fragment has been most frequently observed in the chemistry of molybdenum derivatives, *e.g.* in heterometallic[13,14] anionic $[Mo_2O_2(OMe)\{S(CH_2)_3S\}_3]^-$[15] or neutral homo- $[Cl_2OMo(\mu\text{-}OEt)_2(\mu\text{-}EtOH)MoOCl_2]$[16] or hetero-metallic $[(MeO)_2OMo(\mu\text{-}OMe)_3ReO(OMe)_2]$[17] cluster fragments. As a particular feature of **1** the slightly shorter Mo···Mo distance [2.6545(7) Å] in comparison with those observed for the above-mentioned analogs [2.875(1),[15] 2.683–2.697[16] and 2.658(2)[17] Å] should be mentioned. It can be explained by the fact that in this case the cluster fragment is incorporated into the structure of a polymer which in its turn should reduce the contribution of additional π interaction of the molybdenum atom orbitals with those of oxygen atoms of terminal alkoxide groups. The presence of this

Table 2 Crystal data and the details of diffraction experiments for compounds **1**, **4** and **7**

	1	**4**	**7**
Formula	$C_8H_{25}LiMo_2O_{10}$	$C_{30}H_{70}Li_2Mo_4O_{20}$	$C_{30}H_{74}Li_4O_{43}W_8$
M	480.1	1148.6	2621.5
Crystal system	Monoclinic	Monoclinic	Triclinic
Space group	$P2_1/c$	$P2_1/n$	$P\bar{1}$
a/Å	8.449(2)	11.535(6)	11.461(5)
b/Å	14.256(3)	18.802(8)	11.828(4)
c/Å	14.223(3)	11.673(5)	12.623(5)
α/°			89.90(3)
β/°	97.33(3)	111.11(2)	110.73(3)
γ/°			103.01(3)
U/Å^3	1699.1(6)	2362(2)	1554(1)
T/K	293	157	293
Z	4	2	1
D_c/g cm^{-3}	1.877	1.615	2.802
F(000)	960	1168	1202
μ/cm^{-1}	15.15	11.05	148.4
T_{min}, T_{max}			0.246, 0.983
Absorption correction			ψ Scans
Diffractometer	Enraf-Nonius CAD4	Siemens P3/PC	Enraf-Nonius CAD4
$2\theta_{max}$/°	58	40	60
Scan mode	θ −5 to 3θ	θ–2θ	θ–5/3θ
h,k,l Range	$+h$, $+k$, $\pm l$	$+h$, $+k$, $\pm l$	$+h$, $\pm k$, $\pm l$
Check reflection variation (%)	2.0	1.5	2.0
Number of measured reflections	5049	5601	8628
Number of independent reflections	4496	5297	8192
Number of observed reflections	3085 [$I \geqslant 2\sigma(I)$]	4305 [$I \geqslant 3\sigma(I)$]	5988 [$I \geqslant 2\sigma(I)$]
Number of parameters refined	290	393	388
$R1$ [a]	0.0337	0.0299	0.0591
$wR2$ [b]	0.1030	— [d]	0.1761
R' [c]	—	0.0420	—
Goodness of fit	1.24	1.05	0.98
Maximum Δ/σ ratio	0.19	2.03	0.01
Maximum, minimum residual electron density/e Å^{-3}	0.90, −0.91	0.87, −0.94	1.705, −1.568

Graphite-monochromated Mo-Kα radiation (λ 0.710 73 Å). [a] $\Sigma||F_o| - |F_c||/\Sigma(F_o)$ for observed reflections. [b] $[\Sigma w(F_o^2 - F_c^2)^2/\Sigma w(F_o^2)^2]^{\frac{1}{2}}$ for all reflections. [c] $[\Sigma w(|F_o| - |F_c|)^2/\Sigma w F_o^2]^{\frac{1}{2}}$ for observed reflections. [d] Structure was refined against F; no $wR2$ value was calculated.

effect is reflected in the values of the Mo–O–C bond angles for the 'terminal alkoxo groups' [O(5), O(6), O(7), O(9)] which in the structure of **1** are regularly lower [128.1(3)–130.2(4)°] than those, for example, in the structure of $[MoO(OMe)_4]$ [130.7(6)–137.2(6)°],[6] where the additional π interaction plays a very significant role.

As well as in the structures of the analogous fragments [15–17] all the Mo(1)–μ_2-O(R)–Mo(2) bridges in compound **1** are practically symmetric with their lengths falling in the interval usually observed. The lengths of the bonds formed by oxygen atoms not affected by *trans* influence such as O(1) [Mo(1)–O(1) 2.108(3), Mo(2)–O(1) 2.102(3) Å] and O(3) [Mo(1)–O(3) 2.070(3), Mo(2)–O(3) 2.072(3) Å] are slightly shorter than those in the Mo(1)–O(2)–Mo(2) bridge [Mo(1)–O(2) 2.132(3), Mo(2)–O(2) 2.154(3) Å] elongated due to the *trans* influence of the oxygens O(4) and O(8). The Mo(1)–μ-O(R)–Mo(2) angles are smaller in **1** (76.6–79.7°) than in the structures of the analogs (for example, 84.4° in ref. 15) due, presumably, to the shorter Mo···Mo distance. The bonds which can be considered as 'terminal' for the $Mo_2O_2(OMe)_7$ fragment [Mo(1)–O(5) 1.963(3), Mo(1)–O(6) 1.944(3), Mo(2)–O(7) 1.961(3), Mo(2)–O(9) 1.949(3) Å] are noticeably longer than terminal bonds in the structures of stereochemically isolated fragments (1.895–1.904 Å in that of an isoelectronic molecule [17]) which demonstrates the relative character of the subdivision of the structure of **1** into ionic fragments and indicates predominantly the covalent nature of bonding within the polymer, in spite of the fact that Li–O(Mo) bond lengths in **1** (2.075–2.130 Å) are close to the sum of the correspondent ionic radii (2.08 Å for five-co-ordinated lithium according [18]).

The co-ordination polyhedron of the lithium atom in compound **1** is a tetragonal pyramid. The Li(1) atom is displaced by 0.53(9) Å from the basal plane of the pyramid, O(5)O(6)O(7B)-O(9B), towards the oxygen atom of the MeOH molecule O(10), occupying the axial position and forming the shortest [Li(1)–O(10) 1.972(9) Å] of all Li–O contacts; other Li–O distances are in the range 2.075–2.130 Å. The lithium atom bonded only to the O atoms of alkoxide groups and solvating alcohol molecules usually displays a tetrahedral co-ordination as observed in the structures of $[LiNbO(OEt)_4(EtOH)]$,[19] $[LiNb(OEt)_6]$,[20] $[Li_2Ti_2(OPr^i)_{10}]$,[21] $[LiZr_2(OPr^i)_9(Pr^iOH)]$.[22] The higher co-ordination of lithium in **1** is apparently due to the lower size of the methoxide ligand. An interesting feature of the structure is that the polymeric molecule is built up of alternating $M(\mu\text{-}OR)_2M$ and $M(\mu\text{-}OR)_3M$ elements. The majority of the known polymeric structures of bimetallic alkoxides contain fragments of only one type, for example $[\{LiNb(OEt)_6\}_n]$ features only $M(\mu\text{-}OR)_2M$,[20] whereas $[\{KSn(OBu^t)_3\}_n]$ only $M(\mu\text{-}OR)_3M$.[23] In combination, apart from the structure of **1**, these two different fragments are present also in the structure of $[LaNb_2(OPr^i)_{13}]$,[19] where the lanthanum and one niobium atom form a binuclear $\{LaNbO_9\}$ fragment, while the other niobium atom is connected to lanthanum *via* two Nb–O–La bridges thus forming a four-membered $LaNbO_2$ ring.

The structure of compound **4** is built up of centrosymmetric dimeric $[\{LiMo_2O_4(OPr^i)_4(OC_2H_4OMe)\}_2]$ molecules (Fig. 2, Table 4), and is a combination of a pair of identical triangular fragments that belong to a very widespread $[M_3(\mu_3\text{-}L)_2(\mu\text{-}L')_{2-3}]$ (L, L′ = O or OR) type known for both homo-, as $[Ti_3O(OMe)(OPr^i)_9]$ [24] and $[Ce_3O(OPr^i)_{10}]$,[25] and hetero-metallic alkoxides, $[BaTi_2(OEt)_{10}(EtOH)_5]$,[26] $[LiZr_2(OPr^i)_9(Pr^iOH)]$,[22] *etc.* The skeleton of the triangular fragment is severely distorted. Thus for the Mo–μ-O(R) distances no decrease is observed when we go from the tridentate [Mo(1)–O(5) 2.055(2), Mo(1)–O(7) 2.175(2), Mo(2)–O(5) 2.273(2), Mo(2)–O(7) 2.245(2) Å] to the bidentate groups [Mo(1)–O(6) 2.280(2), Mo(2)–O(6) 1.996(3), Mo(2)–O(10) 1.948(2) Å], while the Mo–O(R) terminal bonds [Mo(1)–O(9), 1.878(2) Å] are nevertheless shorter than any of

Table 3 Selected bond lengths (Å) and angles (°) in compound **1***

Mo(1)–O(4)	1.692(3)	Mo(2)–O(3)	2.072(3)
Mo(1)–O(6)	1.944(3)	Mo(2)–O(1)	2.102(3)
Mo(1)–O(5)	1.963(3)	Mo(2)–O(2)	2.154(3)
Mo(1)–O(3)	2.070(3)	Li(1)–O(10)	1.972(9)
Mo(1)–O(1)	2.108(3)	Li(1)–O(6)	2.075(9)
Mo(1)–O(2)	2.132(3)	Li(1)–O(5)	2.080(9)
Mo(1)···Mo(2)	2.6545(7)	Li(1)–O(7B)	2.103(9)
Mo(2)–O(8)	1.681(3)	Li(1)–O(9B)	2.130(9)
Mo(2)–O(9)	1.949(3)	Li(1A)–O(7)	2.103(9)
Mo(2)–O(7)	1.961(3)	Li(1A)–O(9)	2.130(9)
O(4)–Mo(1)–O(6)	106.7(2)	O(10)–Li(1)–O(6)	103.1(4)
O(4)–Mo(1)–O(5)	104.9(2)	O(10)–L(1)–O(5)	107.1(4)
O(6)–Mo(1)–O(5)	78.94(14)	O(6)–Li(1)–O(5)	73.4(3)
O(4)–Mo(1)–O(3)	93.97(14)	O(10)–Li(1)–O(7B)	106.4(4)
O(6)–Mo(1)–O(3)	87.55(13)	O(6)–Li(1)–O(7B)	150.5(5)
O(5)–Mo(1)–O(3)	159.24(14)	O(5)–Li(1)–O(7B)	99.4(4)
O(4)–Mo(1)–O(1)	90.4(2)	O(10)–Li(1)–O(9B)	102.0(4)
O(6)–Mo(1)–O(1)	160.74(14)	O(6)–Li(1)–O(9B)	100.5(4)
O(5)–Mo(1)–O(1)	88.31(13)	O(7″)–Li(1)–O(9B)	71.7(3)
O(3)–Mo(1)–O(1)	100.26(11)	C(1)–O(1)–Mo(2)	123.6(3)
O(4)–Mo(1)–O(2)	152.66(14)	C(1)–O(1)–Mo(1)	124.0(3)
O(6)–Mo(1)–O(2)	95.30(13)	Mo(2)–O(1)–Mo(1)	78.17(10)
O(5)–Mo(1)–O(2)	94.93(14)	C(2)–O(2)–Mo(1)	124.0(3)
O(3)–Mo(1)–O(2)	70.50(11)	Mo(1)–O(2)–Mo(2)	76.55(10)
O(1)–Mo(1)–O(2)	71.26(12)	C(3)–O(3)–Mo(1)	122.5(3)
O(8)–Mo(2)–O(9)	105.6(2)	C(3)–O(3)–Mo(2)	123.9(3)
O(8)–Mo(2)–O(7)	105.5(2)	Mo(1)–O(3)–Mo(2)	79.71(10)
O(9)–Mo(2)–O(7)	78.69(14)	C(5)–O(5)–Mo(1)	129.8(4)
O(8)–Mo(2)–O(3)	92.3(2)	C(5)–O(5)–Li(1)	126.8(5)
O(9)–Mo(2)–O(3)	88.26(12)	Mo(1)–O(5)–Li(1)	103.2(3)
O(8)–Mo(2)–O(1)	91.0(2)	C(6)–O(6)–Mo(1)	128.5(3)
O(9)–Mo(2)–O(1)	161.01(14)	C(6)–O(6)–Li(1)	121.8(4)
O(3)–Mo(2)–O(2)	70.02(12)	Mo(1)–O(6)–Li(1)	104.0(3)
O(1)–Mo(2)–O(2)	70.93(12)	C(7)–O(7)–Mo(2)	130.2(4)

* Letters A and B denote the atoms derived from the reference atoms by the symmetry operations $x + 1, y, z$ and $x - 1, y, z$ respectively.

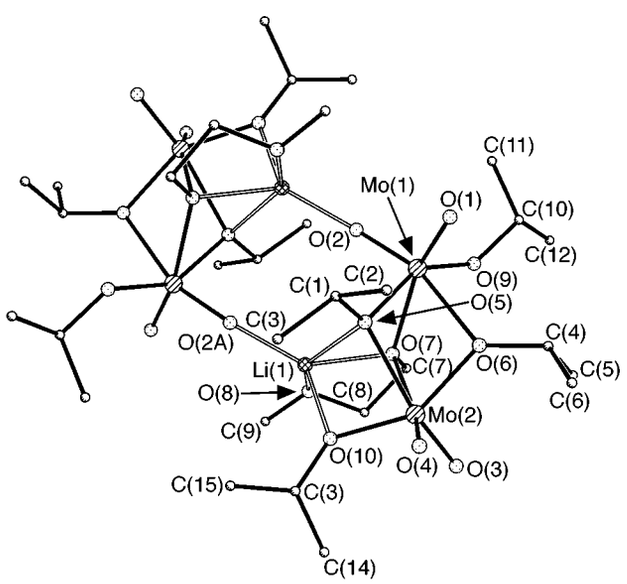

Fig. 2 Structure of the centrosymmetric dimer in the crystal of compound **4**. Only one carbon atom is shown for each of the Pr^i groups; letter A denotes atoms related to the corresponding reference atoms by inversion

the Mo–O(R) bridging distances. The difference in the lengths of the bonds of the same kind is caused apparently by the *trans* influence of the oxygen atoms which appear as terminal ligands for the triangular fragment, and the small size of the lithium atom. The same kind of distortion is observed in the structure of $[\{NaMo_2O_4(OPr^i)_5(Pr^iOH)\}_2]$,[13] which is the closest structural analog of **4**. The Mo–O distances in **4** fall within the range usually observed and the MoO_6 octahedra show minor distor-

Table 4 Selected bond lengths (Å) and angles (°) for compound **4***

Mo(1)–O(1)	1.696(2)	Mo(2)–O(6)	1.996(3)
Mo(1)–O(2)	1.725(2)	Mo(2)–O(7)	2.245(2)
Mo(1)–O(9)	1.878(2)	Mo(2)–O(10)	1.948(2)
Mo(1)–O(5)	2.055(2)	Li(1)–O(8)	2.020(5)
Mo(1)–O(6)	2.280(2)	Li(1)–O(10)	1.969(5)
Mo(1)–O(7)	2.175(2)	Li(1)–O(5)	2.479(5)
Mo(2)–O(3)	1.705(3)	Li(1)–O(7)	1.990(6)
Mo(2)–O(4)	1.696(2)	Li(1)–O(2A)	1.903(5)
Mo(2)–O(5)	2.273(2)	O(2)–Li(1A)	1.903(5)
O(1)–Mo(1)–O(2)	103.7(1)	O(7)–Li(1)–O(8)	82.8(2)
O(1)–Mo(1)–O(5)	98.8(1)	O(5)–Li(1)–O(10)	75.3(2)
O(2)–Mo(1)–O(5)	95.2(1)	O(7)–Li(1)–O(10)	84.0(2)
O(1)–Mo(1)–O(6)	88.6(1)	O(8)–Li(1)–O(10)	103.9(2)
O(2)–Mo(1)–O(6)	162.3(1)	O(5)–Li(1)–O(2A)	105.5(2)
O(5)–Mo(1)–O(6)	70.0(1)	O(7)–Li(1)–O(2A)	142.6(3)
O(1)–Mo(1)–O(7)	158.3(1)	O(8)–Li(1)–O(2A)	100.6(2)
O(5)–Mo(1)–O(7)	68.6(1)	O(10)–Li(1)–O(2A)	129.7(3)
O(6)–Mo(1)–O(7)	70.8(1)	Mo(1)–O(2)–Li(1A)	156.6(2)
O(1)–Mo(1)–O(9)	100.1(1)	Mo(1)–O(5)–Mo(2)	97.5(1)
O(2)–Mo(1)–O(9)	103.1(1)	Mo(1)–O(5)–Li(1)	93.6(1)
O(5)–Mo(1)–O(9)	149.6(1)	Mo(2)–O(5)–Li(1)	78.0(1)
O(3)–Mo(2)–O(4)	104.3(1)	Mo(1)–O(5)–C(1)	121.8(2)
O(3)–Mo(2)–O(5)	157.6(1)	Mo(2)–O(5)–C(1)	130.7(2)
O(4)–Mo(2)–O(5)	97.5(1)	Li(1)–O(5)–C(1)	122.9(2)
O(3)–Mo(2)–O(6)	98.6(1)	Mo(1)–O(6)–Mo(2)	99.0(1)
O(4)–Mo(2)–O(6)	102.2(1)	Mo(1)–O(6)–C(4)	127.2(2)
O(5)–Mo(2)–O(6)	71.1(1)	Mo(2)–O(6)–C(4)	131.8(2)
O(6)–Mo(2)–O(7)	74.7(1)	Mo(1)–O(7)–Mo(2)	94.9(1)
O(3)–Mo(2)–O(7)	94.7(1)	Mo(1)–O(7)–Li(1)	105.6(2)
O(4)–Mo(2)–O(7)	161.1(1)	Mo(2)–O(7)–Li(1)	89.8(1)
O(5)–Mo(2)–O(7)	63.7(1)	Mo(1)–O(7)–C(7)	124.6(2)
O(5)–Mo(2)–O(10)	80.8(1)	C(8)–O(8)–C(9)	113.5(3)
O(6)–Mo(2)–O(10)	147.2(1)	Mo(1)–O(9)–C(10)	129.8(2)
O(7)–Mo(2)–O(10)	78.0(1)	Mo(2)–O(10)–Li(1)	99.7(2)
O(5)–Li(1)–O(7)	63.4(2)	Mo(2)–O(10)–C(13)	125.8(2)
O(5)–Li(1)–O(8)	146.2(3)	Li(1)–O(10)–C(13)	132.4(3)

* Letter A denotes the atoms derived from the reference atoms by the symmetry operation $-x, 1 - y, -z$.

tion, the sums of the bond lengths in *trans* position to each other differing insignificantly: 3.871–4.005 Å for Mo(1) and 3.941–3.978 Å for Mo(2). The stronger distortion of the Mo(1) octahedron is apparently associated with the co-ordination of O(2) by the lithium atom of the neighbouring fragment. The Mo(1)–O(2) bond length in **4** [1.725(2) Å] practically coincides with that observed for the sodium analog [Mo–O(Na) 1.722 Å], which in combination with the observed short alkali metal atom–oxo-oxygen atom distances [Li–O(2) 1.903(5), Na–O 2.256(3) Å], being significantly shorter than the sums of corresponding atomic radii (2.08 and 2.49 Å[18] respectively), demonstrates that the Mo=O bond is sufficiently active to co-ordinate the sodium and lithium atoms. The multiple character of bonding is preserved which is shown not only by the short Mo–O distance but also by the decreased value of the Li(1)–O(2)–Mo(1) angle value, 156.6(2)°. In the structure of $[\{ZnTa_2IO_2(OPr^i)_7\}_2]$, where the triangular $IZnTa_2(\mu_3\text{-}O)(\mu\text{-}OR)_3(OR)_4O$ fragments are also connected *via* an oxygen atom which is in this case disposed symmetrically relative to the tantalum atoms of different fragments, the Ta–(μ-O)–Ta angle is as large as 175.3(5)°.[27] The lithium atom co-ordination in **4** seems to be rather irregular and even if the atom O(5), forming the weakest and presumably 'forced' contact with it, is excluded from consideration, the environment of Li(1) can hardly be treated as a distorted tetrahedron. The O–Li–O angles vary within the limits of 63.4–146.2° (see Table 4), the Li–O bond lengths falling into the range 1.903–2.020 Å. Only one lithium atom contact in the structure of **4** [Li(1)–O(7)] is close to the sum of ionic radii (for tetrahedrally co-ordinated lithium), while two contacts [Li(1)–O(2A) and Li(1)–O(10)] are significantly shorter. This fact in combination with the influence on the bonding parameters of the oxygen atoms connected to lithium indicates

Table 5 Selected bond lengths (Å) and angles (°) in compound **7***

W(1)–O(2)	1.720(8)	W(4)–O(13)	1.701(11)	W(2)–O(20)	1.929(8)	Li(1)–O(2)	2.09(2)
W(1)–O(1)	1.725(8)	W(4)–O(17)	1.899(9)	W(2)–O(21)	1.935(8)	Li(1)–O(12)	2.10(2)
W(1)–O(7A)	1.952(8)	W(4)–O(16)	1.904(9)	W(2)–O(22)	2.323(1)	Li(2)–O(4)	1.91(2)
W(1)–O(5)	1.971(8)	W(4)–O(14)	1.909(10)	W(3)–O(19)	1.708(9)	Li(2)–O(7)	1.98(2)
W(1)–O(3A)	2.140(7)	W(4)–O(15)	1.929(9)	W(3)–O(21)	1.922(8)	Li(2)–O(6)	2.05(2)
W(1)–O(3)	2.179(7)	W(4)–O(22)	2.317(1)	W(3)–O(14B)	1.926(10)	Li(2)–O(5)	2.10(2)
W(2)–O(18)	1.695(9)	Li(1)–O(9)	2.00(2)	W(3)–O(20B)	1.926(8)	Li(2)–O(8)	2.19(2)
W(2)–O(15)	1.916(9)	Li(1)–O(10)	2.02(3)	W(3)–O(16)	1.929(10)	Li(2)–O(3)	2.64(2)
W(2)–O(17B)	1.925(10)	Li(1)–O(11)	2.04(2)	W(3)–O(22)	2.327(1)	O(3)–C(1)	1.458(11)
O(2)–W(1)–O(1)	103.7(4)	O(11)–Li(1)–O(12)	79.2(8)	O(15)–W(2)–O(21)	86.9(4)	W(1A)–O(3)–Li(2)	91.4(5)
O(2)–W(1)–O(7A)	98.1(4)	O(2)–Li(1)–O(12)	94.4(9)	O(17B)–W(2)–O(21)	87.1(4)	W(1)–O(3)–Li(2)	92.6(5)
O(1)–W(1)–O(7A)	92.5(4)	O(4)–Li(2)–O(7)	127.7(11)	O(20)–W(2)–O(21)	152.9(3)	C(3)–O(4)–C(2)	114.4(10)
O(2)–W(1)–O(5)	92.9(4)	O(4)–Li(2)–O(6)	117.6(11)	O(18)–W(2)–O(22)	179.5(4)	C(3)–O(4)–Li(2)	125.0(11)
O(1)–W(1)–O(5)	97.9(4)	O(7)–Li(2)–O(6)	113.5(10)	O(15)–W(2)–O(22)	76.3(3)	C(2)–O(4)–Li(2)	108.8(9)
O(7A)–W(1)–O(5)	162.6(3)	O(4)–Li(2)–O(5)	105.3(11)	O(17B)–W(2)–O(22)	75.7(3)	C(4)–O(5)–W(1)	128.5(8)
O(2)–W(1)–O(3A)	95.5(3)	O(7)–Li(2)–O(5)	93.4(9)	O(20)–W(2)–O(22)	76.5(2)	C(4)–O(5)–Li(2)	104.9(9)
O(1)–W(1)–O(3A)	160.1(3)	O(6)–Li(2)–O(5)	80.3(8)	O(21)–W(2)–O(22)	76.4(2)	W(1)–O(5)–Li(2)	118.5(6)
O(7A)–W(1)–O(3A)	79.2(3)	O(4)–Li(2)–O(8)	91.3(9)	O(19)–W(3)–O(21)	102.9(4)	C(6)–O(6)–C(5)	113.8(11)
O(5)–W(1)–O(3A)	86.4(3)	O(7)–Li(2)–O(8)	78.1(9)	O(9)–Li(1)–O(10)	80.7(9)	C(6)–O(6)–Li(2)	122.5(11)
O(2)–W(1)–O(3)	163.1(3)	O(6)–Li(2)–O(8)	89.9(9)	O(9)–Li(1)–O(11)	97.8(11)	C(5)–O(6)–Li(2)	110.7(10)
O(1)–W(1)–O(3)	92.7(3)	O(5)–Li(2)–O(8)	163.3(11)	O(10)–Li(1)–O(11)	122.9(11)	C(8)–O(8)–Li(2)	109.8(9)
O(7A)–W(1)–O(3)	85.0(3)	O(4)–Li(2)–O(3)	75.5(7)	O(9)–Li(1)–O(2)	96.0(9)	C(11)–O(9)–C(12)	116.2(12)
O(5)–W(1)–O(3)	80.7(3)	O(7)–Li(2)–O(3)	67.0(6)	O(10)–Li(1)–O(2)	124.5(12)	C(11)–O(9)–Li(1)	113.9(11)
O(3A)–W(1)–O(3)	68.7(3)	O(6)–Li(2)–O(3)	148.1(11)	O(11)–Li(1)–O(2)	112.5(12)	C(12)–O(9)–Li(1)	123.7(12)
O(18)–W(2)–O(15)	104.1(5)	O(5)–Li(2)–O(3)	68.0(6)	O(9)–Li(1)–O(12)	169.5(12)	C(10)–O(10)–Li(1)	110.0(12)
O(18)–W(2)–O(17B)	103.8(5)	O(8)–Li(2)–O(3)	120.0(9)	O(10)–Li(1)–O(12)	92.5(10)	C(14)–O(11)–Li(1)	114.9(10)
O(15)–W(2)–O(17B)	152.1(4)	W(1)–O(2)–Li(1)	141.9(7)	C(7)–O(7)–W(1A)	127.8(8)	C(15)–O(11)–Li(1)	124.4(11)
O(18)–W(2)–O(20)	103.6(4)	C(1)–O(3)–W(1A)	125.1(6)	C(7)–O(7)–Li(2)	106.8(9)	C(13)–O(12)–Li(1)	105.6(10)
O(15)–W(2)–O(20)	86.7(4)	C(1)–O(3)–W(1)	121.5(5)	W(1A)–O(7)–Li(2)	121.9(7)	W(2)–O(15)–W(4)	117.3(4)
O(17B)–W(2)–O(20)	86.4(4)	W(1A)–O(3)–W(1)	111.3(3)	C(9)–O(8)–Li(2)	131.5(11)	W(4)–O(22)–W(2)	90.11(3)
O(18)–W(2)–O(21)	103.4(4)	C(1)–O(3)–Li(2)	99.7(7)				

* Letters A and B denote the atoms derived from the reference atoms by the symmetry operations $-x-1$, $-y+1$, $-z$ and $-x$, $-y$, $-z-1$ respectively.

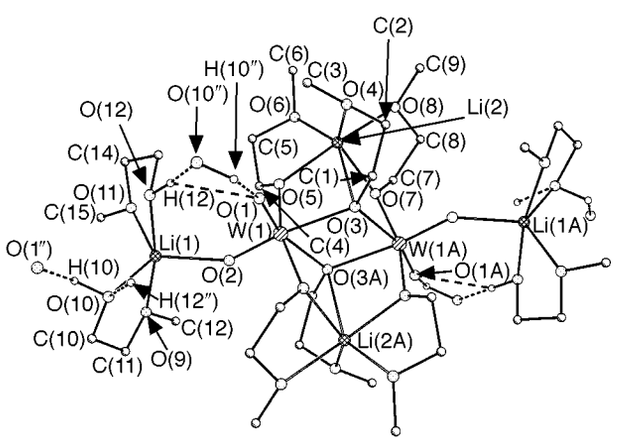

Fig. 3 Structure of the cationic aggregates $[\{LiWO_2(OC_2H_4OMe)_3\}_2 \cdot 2Li(HOC_2H_4OMe)_2]^{2+}$ in the crystal of compound **7**. The atoms derived from the corresponding reference atoms by $x-1$, y, z and $-x$, $1-y$, $-z$ symmetry operations are primed and doubly primed respectively; those that are related to the corresponding atoms by inversion are denoted by letter A

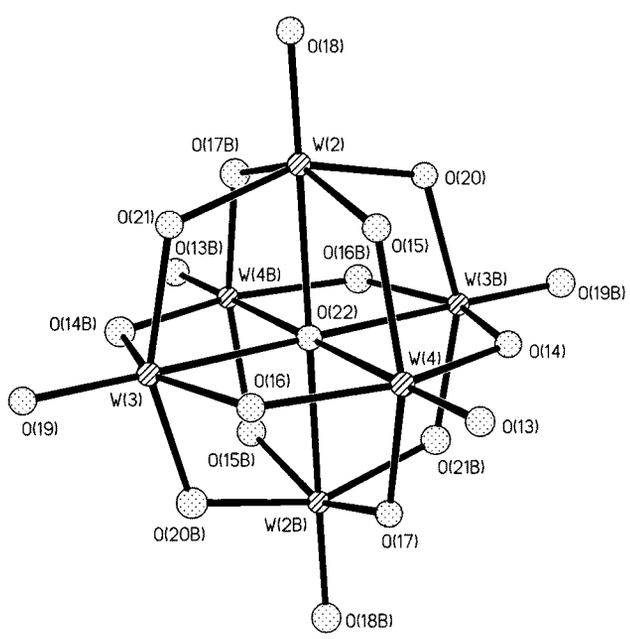

Fig. 4 Structure of the $[W_6O_{19}]^{2-}$ anion in the crystal of compound **7**. Letters A and B denote atoms derived from the reference atoms by the symmetry operations $-x-1$, $-y+1$, $-z$ and $-x$, $-y$, $-z-1$ respectively

the predominantly covalent character of its bonding with the neighbouring atoms.

In the structure of compound **7**, $[\{LiWO_2(OC_2H_4OMe)_3\}_2 \cdot 2Li(HOC_2H_4OMe)_2]^{2+}[W_6O_{19}]^{2-}$, one neutral centrosymmetric $\{Li_2W_2O_4(OR)_6\}$ and two cationic $\{Li(ROH)_2\}^+$ fragments are bound by W=O–Li bonds [Li(1)–O(2) 2.09(2) Å] into hexanuclear cationic aggregates of $[\{Li_2W_2O_4(OR)_6\}\{Li(ROH)_2\}_2]^{2+}$ composition, $R = OC_2H_4OMe$ (Fig. 3, Table 5), which are linked *via* O(10)–H(10)···O(1″) ($-x$, $1-y$, $-z$) hydrogen bonds into infinite zigzag chains stretching along the *a* axis [O(10)···O(1″) 2.75(1) Å]. There are also two more rather long contacts involving the H(12) atom, one of them corresponding to the intramolecular [O(12)···O(1) 3.02(1) Å] and another corresponding to the intermolecular [O(12)···O(10″) 3.12(1) Å] hydrogen bonds.

The $[W_6O_{19}]^{2-}$ ion has a centrosymmetric structure (Fig. 4), tungsten atoms forming an octahedral $\{W_6\}$ framework, centered with the μ_6-oxygen atom O(22) and made up of six edge-sharing WO_6 octahedra. The W–μ_6-O distances [W(2)–O(22) 2.323(1), W(3)–O(22) 2.327(1), W(4)–O(22) 2.317(1) Å] and overall geometry of the anion are in good agreement with

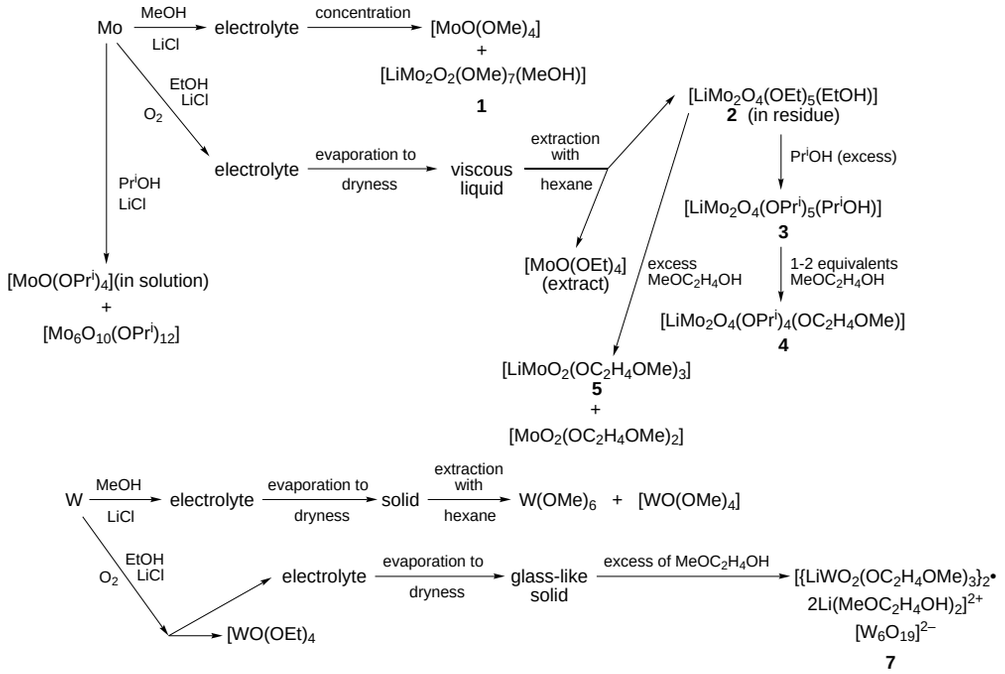

Scheme 1

those found in the structure of $[NBu_4]_2[W_6O_{19}]$[28] [W–μ_6-O 2.311(1)–2.328(1) Å]. The lengths of terminal W=O bonds (1.695–1.708 Å) in the structure of the anion of compound **7** are as usual shorter than those of W–μ-O bonds (1.899–1.929 Å) and W–μ_6-O bonds (2.317–2.327 Å). The W=O and W–μ-O bond lengths are similar to the statistical average values for such bonds.[29]

The most important feature of the structure of the $[\{Li_2W_2O_4(OR)_6\}\{Li(ROH)_2\}_2]^{2+}$ cationic aggregate is the W=O–Li bond between the neutral and the cationic fragments. The length of the corresponding bond W(1)–O(2) [1.720(8) Å] practically coincides in this case with that of W(1)–O(1) [1.725(8) Å], involving the O(1) atom participating in a moderately strong hydrogen O(1)···O(10) bond. The average W=O bond length (1.722 Å) for the dicationic fragment of **1** is smaller than that found in WO_2 groups of binuclear anions $[W_2O_6L']^{5-}$ $\{H_5L' = MeC(OH)[PO(OH)_2]_2\}$[30] (1.745 and 1.739 Å), $[W_2O_5L''_2]^{6-}$ $[H_4L'' = HOC(CH_2CO_2H)_2CO_2H]$[31] (1.753 and 1.762 Å), $[W_2O_5(OMe)_4]^{2-}$[32] (average value 1.739 Å). It is important to note that the tungsten atoms in all these compounds are co-ordinated exclusively by oxygen atoms. This should be taken into consideration for correct comparison of terminal W=O bond lengths because the different redistributions of the electron density within the WO_6 co-ordination octahedra of the W atom in various compounds lead to considerable variations in the lengths of bonds which should formally be considered as having the same structural functions. Thus, for example, in the structures of monomeric octahedral complexes $[WO_2Cl_2(OPPh_3)_2]$,[33] $[WO_2Cl_2(OMe_2)]$[34] and $[WO_2F_2(bipy)]$ (bipy = 2,2′-bipyridine)[35] the W=O bond lengths in WO_2 groups are significantly shortened being equal to 1.704, 1.67 and 1.667 Å. At the same time, the W=O bond length in a 'wolframyl' group is to a certain extent dependent upon the nature of other bonds in the co-ordination polyhedron of the tungsten atom. Thus in ref. 29 the elongation of W=O bonds in $[W_2O_6L']^{5-}$ was explained by formation of a pseudo-trioxo group WO_3 (taking into account that one of the W–μ-O bridging bonds is strongly shortened in comparison with the other analogous bridging bonds equal to 1.828 Å), as the W–O bonds should logically be longer in WO_3 groups than in WO_2 due to delocalization of π bonding over three bonds (rather than two bonds as in WO_2).

The co-ordination polyhedron of Li(1) is a trigonal bipyramid, its equatorial plane being formed by O(2), O(10) and O(11) and apical positions occupied by atoms O(9) and O(12) [O(9)–Li(1)–O(12) 169.5(12)°]. The Li(1)–O(2) bond length [2.09(2) Å], responsible for the formation of the cationic aggregate, as well as other Li–O bond lengths (2.00–2.10 Å) are close to the sum of ionic radii for five-co-ordinated Li^+ cation and two-co-ordinate O^{2-} anion (2.04 Å[12]).

In contrast to the co-ordination polyhedron of Li(1) with long bonds indicating their predominantly ionic character, in the Li(2) co-ordination polyhedron there is one considerably shortened Li(2)–O(4) bond [1.91(2) Å]. The co-ordination polyhedron can hardly be associated with any of the regular geometries known for six-co-ordinated atoms: the minimum and maximum bond angles are 67.0(6) and 163.3(11)° respectively (see Table 5). This is apparently due to both very mild co-ordination requirements of Li and the steric tension arising on formation of the chelate rings.

The structure of the $\{Li_2M_2O_6\}$ core of the neutral bimetallic $[Li_2W_2O_4(OR)_6]$ fragment belongs to the $[\{Ti(OR)_4\}_4]$ type (R = Me or Et[36]) quite frequently found in the metal alkoxide structures. The core formed by atoms Li(2), Li(2A), W(1), W(1A), O(3), O(3A), O(5), O(5A), O(7), O(7A) is not planar: the central W(1)O(3)W(1A)O(3A) ring is rotated by 62.7(3)° relative to the W(1)Li(2)W(1A)Li(2A) plane. Among the known structures of the bimetallic alkoxides the analogous metal–oxygen frameworks have been observed for $NaMO_2(O-C_2H_4OMe)_3$, M = Mo[10] or W,[14] where the dimeric molecules were also built up of two octahedra sharing a common edge. In contrast to compound **7** where the W–O–W bridges are nearly symmetric (W–O 2.140 and 2.179 Å), the Mo–O–Mo bridges in $[NaMoO_2(OC_2H_4OMe)_3]$ (Mo–O 2.255 and 2.162 Å) are significantly asymmetric. The apparent analogy in structure and composition of the considered fragment and the known bimetallic 2-methoxyethoxides allows to suggest that the complex **5** possesses an analogous molecular structure.

Conditions of formation and isolation of the side products of electrosynthesis

The present study showed cathodic reduction to be a general characteristic feature of electrosynthesis (see Scheme 1), having a more pronounced effect in case of tungsten than of molybdenum. Its extent increases if the same metal is used as cathode

and at higher concentrations of conductive additive. The product obtained in the anodic oxidation of molybdenum in Pr^iOH revealed the highest stability to oxidation. Its IR spectrum and chemical properties testified to its identity with $[Mo_6O_{10}(OPr^i)_{12}]$ **6**, earlier obtained by Chisholm *et al.*[9] by oxidation of $Mo_2(OPr^i)_8$ with molecular oxygen. This was quite surprising taking into account the usual stability of methoxides and the reluctance of methanol to participate in side reactions that in the case of molybdenum dissolution in methanol resulted in isolation of a comparably stable compound **1**, which proved to be a bimetallic compound of lithium and Mo^V formally derived from the $MoO(OR)_3$ series, which has not been described in the literature as far as we know. It is interesting that the product of cathodic reduction of tungsten methoxide in MeOH is immediately oxidized on attempted isolation and the resulting mixture of products consists of $W(OMe)_6$ and $[WO(OMe)_4]$. We failed, unfortunately, to identify the bimetallic complexes formed *in situ* on dissolution of metals in EtOH because of the extremely strong trend of ethoxo-molybdates and -tungstates(v) to oxidation. Therefore, the products of their reaction with molecular oxygen were analysed. In the case of molybdenum, after extraction of $[MoO(OEt)_4]$, from the residue the product to which the composition $[LiMo_2O_4(OEt)_5(EtOH)]$ **2** was ascribed was practically quantitatively crystallized (unfortunately, twinning problems hindered X-ray single-crystal studies). The composition of **2** was confirmed indirectly by the results of an X-ray study of the product of its treatment with an excess of Pr^iOH and controlled amounts of 2-methoxyethanol, equation (4).

$$\underset{\mathbf{2}}{[LiMo_2O_4(OEt)_5(EtOH)]} \xrightarrow{Pr^iOH\ (excess)} \underset{\mathbf{3}}{[LiMo_2O_4(OPr^i)_6(Pr^iOH)]} \xrightarrow{1\text{–}2\ equivalents\ MeOC_2H_4OH} \underset{\mathbf{4}}{[LiMo_2O_4(OPr^i)_4(OC_2H_4OMe)]} \quad (4)$$

Compound **4**, easily crystallizable from hexane, results from substitution of one of the OPr^i groups in **3** with a 2-methoxyethoxide group. The IR spectra of **2**–**4**, and those of $[NaMo_2O_4(OR)_5(ROH)]$ (R = Et or Pr^i)[7,13] are similar to each other in the ν(M–O) region, which also testifies to the analogy in their structures.

It is interesting that the complete substitution of OR groups in compound **2** with 2-methoxyethoxide ones leads to an equimolar mixture of $[MoO_2(OC_2H_4OMe)_2]$ and $[LiMoO_2(OC_2H_4OMe)_3]$ **5**, equation (5). The isolated complex **5** can also

$$[LiMo_2O_4(OEt)_5(EtOH)] + \underset{(excess)}{MeOC_2H_4OH} \xrightarrow{-EtOH} [MoO_2(OC_2H_4OMe)_2] + \underset{\mathbf{5}}{[LiMoO_2(OC_2H_4OMe)_3]} \quad (5)$$

be prepared by direct interaction of 2-methoxyethoxides of lithium and molybdenum in 2-methoxyethanol, equation (6).

$$[MoO_2(OC_2H_4OMe)_2] + LiOC_2H_4OMe \xrightarrow{ROH} [LiMoO_2(OC_2H_4OMe)_3] \quad (6)$$

Its IR spectrum is very similar to that provided for $[NaMO_2(OC_2H_4OMe)_3]$ (M = Mo[10] or W[14]) thus indicating the analogy in their structure.§ Compound **5** turned out to be rather less stable in comparison with the sodium derivative: it can be present unchanged in solution only in the presence of an excess of $[MoO_2(OC_2H_4OMe)_2]$. If dissolved in pure ROH, or in a solution containing LiOR (R = C_2H_4OMe), it undergoes complete decomposition leading to formation of a mixture of Li_2MoO_4 and $Li_2Mo_2O_7$.

In contrast to the situation observed for molybdenum, the anodic dissolution of tungsten in EtOH leads to two main products, crystalline $[WO(OEt)_4]$ and glass-like $[WO_n(OEt)_{6-2n}]$, where $n \geqslant 2$. The latter is also contaminated by lithium. On the reaction of an excess of 2-methoxyethanol with the residue upon evacuation of the electrolyte $[\{LiWO_2(OC_2H_4OMe)_3\}_2 \cdot 2Li(MeOC_2H_4OH)_2]^{2+}[W_6O_{19}]^{2-}$ **7** was obtained in high yield (>50% in relation to the amount of metal consumed). So the considerable decomposition with formation of oxo complexes is presumably due to the higher extent of cathodic reduction and easier oxidation of the reduced products for tungsten alkoxides in comparison with molybdenum ones.

As the most important result of the present work we consider the identification of bimetallic lithium derivatives among the side products of electrosynthesis. None of the isolated complexes contained chlorine atoms, *i.e.* they were formed due to complexation between molybdenum (or tungsten) alkoxides and LiOR. The latter originated from the following electrochemical reaction (7) analogous to that known for water

$$LiCl + ROH \longrightarrow LiOR + \tfrac{1}{2}H_2\uparrow + Cl^{\bullet} \quad (7)$$

solutions. Oxidation of alcohols by released chlorine radicals should lead, for example, to reactions (8) and (9). A GLC–mass

$$EtOH + 2Cl^{\bullet} \longrightarrow MeCHO + 2HCl \quad (8)$$

$$EtOH + HCl \longrightarrow EtCl + H_2O \quad (9)$$

spectrometric study of methanol-based electrolytes has not indicated the presence of such derivatives (presumably because of their high volatility) but in the case of electrolytes based on EtOH and Pr^iOH they were represented by alkyl halides and aldehydes or ketones (see Table 1). The presence in the electrolyte obtained by anodic oxidation of molybdenum in EtOH of such a specific product as the diethyl acetal of acetaldehyde is presumably due to condensation of the initially formed aldehyde with alcohol, promoted by the catalytic action of $[MoO(OEt)_4]$, equation (10).

$$MeCHO + 2EtOH \xrightarrow{[MoO(OEt)_4]} MeCH(OEt)_2 + H_2O \quad (10)$$

The results obtained permit us also to propose a general preparation scheme for different homologues of the $[MoO(OR)_4]$ series, based on the electrochemical technique: a first step in all cases is the anodic oxidation of metal, for example, in ethanol. It should always be followed by separation of the alkoxide oxide by extraction {as the side products, *i.e.* bimetallic alkoxides of lithium and molybdenum, are more easily separable from the product, $[MoO(OR)_4]$, for R = Et than for R = Pr^i, C_2H_4OMe} and the final step should be the alcohol interchange reaction of the pure $[MoO(OEt)_4]$. An analogous approach can be applied for the preparation of different homologues of the $W(OR)_6$ series, but in this case the reagent for the alcohol-interchange reaction should be $W(OMe)_6$, prepared by anodic oxidation of tungsten in methanol. Alcohol-interchange techniques for preparation of molybdenum and tungsten alkoxides have been described.[7,10,14]

Acknowledgements

The authors express their gratitude to International Science Foundation, Grants MPR 000 and MPR 300, and European Program of Intellectual and Technical Assistance to the Former

§ It should be mentioned that the metal–oxygen core analogous to those of Na–Mo(W) 2-methoxyethoxides was also observed in the structure of a Li–W 2-methoxyethoxide cation (see above).

States of the Soviet Union, Grants 93-2792 and 94-771, and the Russian Foundation for Basic Research, Project 97-03-33783, and Russian Foundation for Fundamental Research for Technological Applications for financial support of this work.

References

1 N. Ya. Turova, E. P. Turevskaya, V. G. Kessler and M. I. Yanovskaya, *J. Sol-Gel Sci. Technol.*, 1994, **2**, 18.
2 E. P. Kovsman, S. I. Andruseva, L. I. Slovjeva, V. I. Fedyaev, M. N. Adamova and T. V. Rogova, *J. Sol-Gel Sci. Technol.*, 1994, **2**, 61.
3 V. A. Shreider, E. P. Turevskaya, N. I. Kozlova and N. Ya. Turova, *Inorg. Chim. Acta*, 1981, **53**, L73.
4 N. Ya. Turova and V. G. Kessler, *Russ. J. Gen. Chem.*, 1990, **60**, 113.
5 S. I. Kucheiko, N. Ya. Turova and V. A. Shreider, *Russ. J. Gen. Chem.*, 1985, **55**, 2396.
6 V. G. Kessler, A. V. Mironov, N. Ya. Turova, A. I. Yanovsky and Yu. T. Struchkov, *Polyhedron*, 1993, **12**, 1573.
7 N. Ya. Turova, V. G. Kessler and S. I. Kucheiko, *Polyhedron*, 1991, **10**, 2617.
8 V. G. Kessler, S. Yu. Vasilyev, A. I. Belokon' and N. Ya. Turova, *Russ. J. Gen. Chem.*, 1990, **60**, 2629.
9 M. H. Chisholm, K. Folting, J. C. Huffman and C. C. Kirkpatrick, *Inorg. Chem.*, 1984, **23**, 1021.
10 V. G. Kessler, N. Ya. Turova, A.V. Korolev, A. I. Yanovsky and Yu. T. Struchkov, *Mendeleev Commun.*, 1991, 89.
11 S. I. Kucheiko, N. Ya. Turova and N. I. Kozlova, *Sov. J. Coord. Chem.*, 1985, **11**, 1521, 1656.
12 SHELXTL PLUS PC, Version 4, Siemens Analytical X-Ray Instruments, Madison, WI, 1990; Version 5, Siemens Industrial Automation, Madison, WI, 1994.
13 V. G. Kessler, N. Ya. Turova, A. I. Yanovsky and Yu. T. Struchkov, *Russ. J. Gen. Chem.*, 1990, **60**, 2769.
14 V. G. Kessler, D. E. Chebukov and N. Ya. Turova, *Russ. J. Inorg. Chem.*, 1993, **18**, 23.
15 L. Ma, S. Liu, H. Zhu and J. Zubieta, *Polyhedron*, 1989, **8**, 669.
16 C. Limberg, S. Parsons, A. J. Downs and D. J. Watkin, *J. Chem. Soc.*, *Dalton Trans.*, 1994, 1169.
17 V. G. Kessler, G. A. Seisenbaeva, A. V. Shevelkov and G. V. Khvorykh, *J. Chem. Soc.*, *Chem. Commun.*, 1995, 1779.
18 R. D. Shannon, *Acta Crystallogr.*, *Sect. A*, 1976, **32**, 751.
19 E. P. Turevskaya, N. Ya. Turova, A. V. Korolev, A. I. Yanovsky and Yu. T. Struchkov, *Polyhedron*, 1995, **14**, 1531.
20 D. Eichorst, D. A. Payne, S. R. Wilson and K. E. Howard, *Inorg. Chem.*, 1990, **29**, 1458.
21 M. J. Hampden-Smith, D. S. Williams and A. L. Rheingold, *Inorg. Chem.*, 1990, **29**, 4076.
22 B. A. Vaarstra, J. C. Huffman, W. E. Streib and K. G. Caulton, *J. Chem. Soc.*, *Chem. Commun.*, 1990, 1750.
23 M. Veith and R. Rosler, *Z. Naturforsch.*, *Teil B*, 1986, **41**, 1071.
24 V. W. Day, D. A. Ebershpaher, Y. Chen, J. Hao and W. J. Klemperer, *Inorg. Chim. Acta*, 1995, **229**, 391.
25 L. G. Hubert-Pfalzgraf and C. Sirio, personal communication.
26 A. I. Yanovsky, E. P. Turevskaya, M. I. Yanovskaya, V. G. Kessler, N. Ya. Turova, A. P. Pissarevsky and Yu. T. Struchkov, *Russ. J. Inorg. Chem.*, 1995, **40**, 355.
27 S. Boulmaaz, L. G. Hubert-Pfalzgraf, S. Halut and J.-C. Daran, *J. Chem. Soc.*, *Chem. Commun.*, 1994, 601.
28 A. I. Yanovsky, S. I. Kucheiko and Yu. T. Struchkov, *Sov. J. Coord. Chem.*, 1987, **13**, 694.
29 *Structure Correlation*, eds. H.-B. Burgi and J. D. Dunitz, VCH, Weinheim, New York, 1994, vol. 2, p. 815.
30 V. S. Sergiyenko, E. O. Tolkacheva and A. B. Ilukhim, *Russ. J. Inorg. Chem.*, 1994, **39**, 243.
31 E. Llopis, J. A. Ramirez, A. Domenech and A. Cervilla, *J. Chem. Soc.*, *Dalton Trans.*, 1993, 1121.
32 W. Clegg, R. J. Errington, K. A. Fraser and D. G. Richards, *J. Chem. Soc.*, *Chem. Commun.*, 1993, 1105.
33 J. F. Wet, M. R. Caira and B. J. Gellatly, *Acta Crystallogr.*, *Sect. B*, 1978, **34**, 762.
34 M. G. B. Drew, G. W. A. Fowles, D. A. Rice and K. J. Shanton, *J. Chem. Soc.*, *Chem. Commun.*, 1974, 64.
35 P. Schreiber, K. Weighardt, B. Nuber and J. Weiss, *Z. Naturforsch.*, *Teil B*, 1990, **45**, 619.
36 J. A. Ibers, *Nature* (*London*), 1963, **197**, 686.

Received 16*th June* 1997; *Paper* 7/04198E